

Trapped ion imaging with a high numerical aperture spherical mirror

G Shu, M R Dietrich, N Kurz and B B Blinov

Department of Physics, University of Washington, Seattle, WA 98105-1560, USA

E-mail: shugang@u.washington.edu

Received 29 January 2009, in final form 12 April 2009

Published 15 July 2009

Online at stacks.iop.org/JPhysB/42/154005

Abstract

Efficient collection and analysis of trapped ion qubit fluorescence is essential for robust qubit state detection in trapped ion quantum computing schemes. We discuss simple techniques of improving photon collection efficiency using high numerical aperture (N.A.) reflective optics. To test these techniques we placed a spherical mirror with an effective N.A. of about 0.9 inside a vacuum chamber in the vicinity of a linear Paul trap. We demonstrate stable and reliable trapping of single barium ions, in excellent agreement with our simulations of the electric field in this setup. While a large N.A. spherical mirror introduces significant spherical aberration, the ion image quality can be greatly improved by a specially designed aspheric corrector lens located outside the vacuum system. Our simulations show that the spherical mirror/corrector design is an easy and cost-effective way to achieve high photon collection rates when compared to a more sophisticated parabolic mirror setup.

(Some figures in this article are in colour only in the electronic version)

1. Introduction

Trapped ion quantum computing is a rapidly progressing and developing area of experimental and theoretical research [1]. All basic building blocks of a quantum information processor based on trapped ions have been demonstrated: qubit initialization, typically via optical pumping; qubit state manipulation by RF [2] or optical [3] fields; qubit state readout by quantum jumps [4]. Fundamental quantum logic gates [5] and multi-qubit entanglement [6, 7] have also been demonstrated. In this paper we address the issue of qubit state readout which is typically based on the ion bright/dark state discrimination. Efficient ion fluorescence collection is critical for fast, reliable qubit state detection required not only at the end of any quantum computation, but throughout the computation process to enable quantum error correction [8, 9]. Additionally, higher photon collection rates from single trapped ions or atoms would lead to more efficient single-photon sources and ion-photon entanglement [10].

Ion fluorescence collection is commonly performed using reasonably high-N.A. refractive optics, achieving a collection efficiency of a few per cent. A major practical limitation in using this type of optics is the large working distance, of order of a few cm, due to the fact that the lens is located outside

the vacuum chamber. High-N.A. optics in this case becomes a very expensive, custom job. Some efforts have been made to place the lens inside the vacuum apparatus, closer to the ion trap [11, 12] to achieve up to about 5% light collection efficiency.

Another approach is to use reflective optics such as an optical cavity, or a single spherical or parabolic mirror. A small (order of 100 μm), high-finesse optical cavity similar to those used in cavity QED experiments [13, 14] appears to be the ultimate solution. Many serious efforts are under way to couple trapped ions to a high-finesse cavity [15, 16] and rapid progress is being made. However, the presence of dielectric cavity mirrors in the close vicinity of the trapped ions may be detrimental to the ion trapping process. A parabolic mirror surrounding the ion trap is an attractive alternative [17]. It would provide excellent performance in terms of image quality. However, making a high-N.A. parabolic mirror itself is quite a demanding task. Our simulations of a parabolic mirror show that it is also sensitive to ion's alignment with respect to the focus of the mirror. A spherical mirror, due to its high symmetry, is much less sensitive to such misalignment.

A spherical mirror placed in the vacuum with ions in the centre of the mirror curvature has been used to double the photon count on a large-area photomultiplier tube [18], but

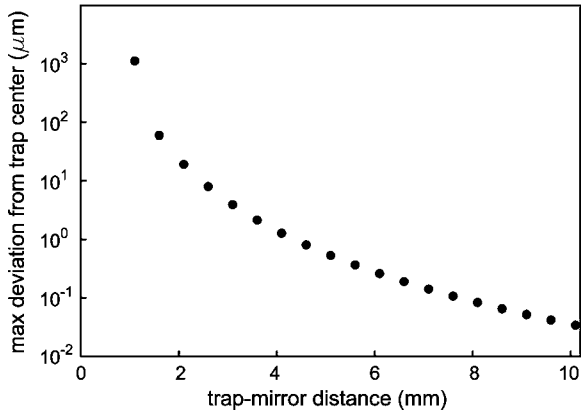


Figure 1. Trapped ion orbit rms displacement from its unperturbed position due to the presence of a grounded metallic surface in the vicinity of the trap as a function of the distance between the trap centre and the surface.

was not used for imaging. Here we present an ion imaging system based on 0.9 N.A. spherical mirror which is in principle capable of collecting up to about 28% of light emitted by the ion. To improve the image quality which suffers greatly from strong spherical aberration introduced by the high-N.A. mirror we designed an aspherical corrector lens based on the widely used Schmidt telescope corrector element. Our simulations show that with this corrector the ion image is suitable not only for high-quality imaging and photon counting, but possibly even for fibre-coupling single ion fluorescence.

2. Simulations of ion trap and optical system

To model the ion trap behaviour in the presence of a spherical mirror we used the method of images [19]. We compared the trapped ion orbit in an unperturbed quadrupole electric field produced by the four RF electrodes of our linear trap, described in much detail in the following section, to the ion motion in the presence of a grounded metallic symmetry plane nearby, which is a simplified model of the spherical metallic mirror. Our simulations show that the ion orbit is perturbed by less than 1 μm if the plane is farther than 5 mm away. This displacement of the trapping centre is negligible and, if necessary, can be easily corrected by applying a small bias voltage to the top RF electrodes. Figure 1 shows the calculated orbit displacement of a trapped ion in the trap in the presence of a spherical mirror.

Due to restrictions imposed by our ion trap construction, the size of the reflective surface is limited to $20 \times 20 \text{ mm}^2$. To achieve the highest numerical aperture, the mirror should stay as close as possible to the trapping centre. Several considerations prevent it from being too close: the mirror should not block the cooling laser access arranged at right angle to the mirror axis, and the entirety of the mirror surface should be shielded from the atomic barium beam to avoid coating. Additionally, it should not significantly affect the trap stability as discussed above. We found a suitable spherical mirror with a focal length of 10 mm in Edmund Optics catalog (stock no. NT43-464) and set out to model its performance.

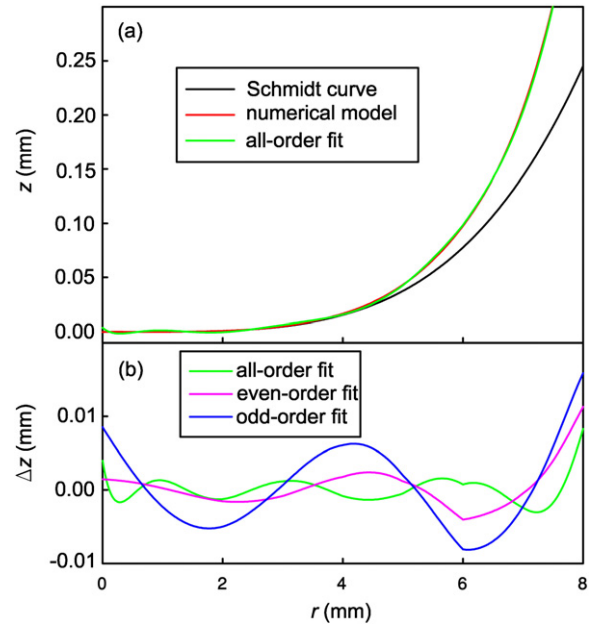


Figure 2. (a) Thickness z of various corrector plate shapes plotted versus distance r from the optical axis: the Schmidt corrector (black), the numerical model curve (red) and the 10th order polynomial fit to the numerical result (green). (b) Deviations of various types of polynomial fits from the exact numerical model. (This figure is in colour only in the electronic version)

2.1. Aspheric corrector lens

Using an aspheric plate to correct the aberration of the image by a spherical mirror was invented by Bernhard Schmidt in 1930 (see e.g. [20]). The concept is to distort the collimated light beam before it hits the mirror to cancel most of the spherical aberration in reflection. This is achieved by adding a piece of optics through which the spherical mirror looks like a parabolic mirror. It is widely used in telescopes and reflective camera lenses. To lowest order, the general corrector curve equation can be expressed as

$$z = \frac{(r^4 - kr^2)d^4}{4(n-1)R^3} \quad (1)$$

where z is the thickness of the corrector, r is the distance from the optical axis, R is the radius of curvature of the spherical mirror, and n is the refractive index of the corrector material. k is a constant determined by the corrector plate's position with respect to the mirror, which is normally within R . In our situation, the problem is reversed: we attempt to create a collimated beam of light emitted by a point source (the ion) reflected from a spherical mirror. An additional restriction is that the view port is about 17 mm away from the mirror focus, so k should be equal to 0, corresponding to a plate at the centre of the mirror curvature. Through this general formula, we arrive at a fourth-order curve equation for our specific parameters (using standard BK7 glass):

$$z = 5.98785 \times 10^{-5} r^4. \quad (2)$$

This curve is plotted in figure 2(a) as the black solid line. However, the fourth-order curve works well only for small N.A. mirrors. In our case, higher order terms (and higher order

aberrations, and aberrations due to the planar view port) would have to be taken into account to determine the optimal corrector shape. For typical systems such as a reflective telescope or a Schmidt camera, better performance can be achieved by adding a small lens between the focus and the mirror, but this would not work for us since the refractive optics placed too close to the trap would destabilize the ion by patch charging.

As an alternative, we tried a brute-force approach by directly calculating the best correcting element shape for our specific setup. The principle is quite simple: ensure that any ray originating from the ion and reflected off the mirror is parallel to the optical axis. Another option would be to make the deflected ray slope proportional to its distance from the main optical axis. We do not attempt to derive a general solution here, rather the one ideal for our application. We used Wolfram Research, Inc. Mathematica to numerically perform the ray tracing and curve fitting. Because of the rotational symmetry, the problem can be reduced to two dimensions. The slopes of the ray span are recursively calculated at the curve vertex z -value and then integrated and expressed as a function of r , the distance from the optical axis. The deviation from the vertex is added to the thickness of the corrector plate for the next round of calculation. The curve equation converged quickly and the difference was smaller than a quarter of the wavelength after only 10 iterations. Again, the standard BK7 glass was used in the simulation.

This numerical simulation predicted an irregular curve shown in figure 2(a) as a red line. We used the optics modelling software (Sinclair Optics, Inc. OSLO LT) to evaluate the performance of such a corrector element. Since OSLO LT only supports polynomials up to order 10 for its surface data input, it was impossible to exactly reproduce the shape of the corrector in the simulation. Instead, we fit the corrector shape profile with even, odd and full 10th order polynomials; they differ by as much as $20\ \mu\text{m}$ (about 40 times the wavelength at $493\ \text{nm}$) from the numerically derived shape. The even-order polynomial fit is very good close to the optical axis but gets much worse than the full 10th order polynomials fit in off-axis region. The odd-order polynomial has the worst fit overall. The all-order polynomial fit is plotted in figure 2(a) in green, and the deviations of the three types of fits from the numerical model are plotted in figure 2(b).

Surprisingly, all of the fits perform much better than the equation (2) curve in correcting the spherical aberration. We estimated the corrector's performance by modelling how well the collimated beam it produces is focused by an infinity-corrected microscope objective [21] (figure 3(a)). As shown in figure 3(b), both the even- and full-order curves gave a root mean square spot size of $67\ \mu\text{m}$, about 1/3 the spot size produced by the 4th order curve in equation (2). With some basic spatial filtering techniques, any background from light scattered from other surfaces and other sources can be largely suppressed so that a PMT can be used for high-speed, accurate photon detections with low noise. If the actual numerically derived corrector shape is used rather than a fit, we believe the performance should be close to that of a perfect parabolic mirror, and nearly diffraction-limited imaging and single-mode fibre coupling should be possible. Off-axis displacement

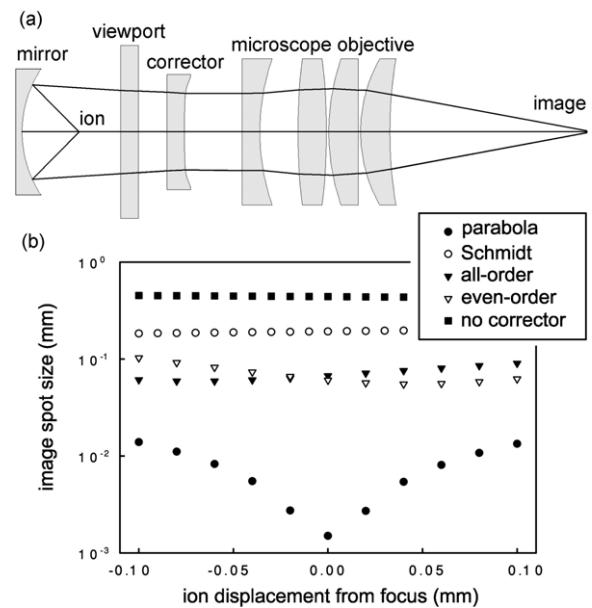


Figure 3. Simulation of the corrector performance. (a) The simulation model. A point source of light is reflected off the spherical mirror and, after passing through a flat viewport window and the corrector plate, is imaged with the microscope objective. To model the parabolic mirror performance the corrector element was taken out. Note that in the preliminary result reported in section 4, the corrector and the multi-element lens were not used. (b) Spot sizes produced by different shape correctors as a function of ion displacement from the focus along the optical axis. The diffraction limit for this setup at $493\ \text{nm}$ is about $1.5\ \mu\text{m}$.

up to $100\ \mu\text{m}$ will increase the spot size by less than 5%, which makes it possible to resolve a string of tens of ions $5\text{--}10\ \mu\text{m}$ apart.

3. Experimental setup

To test the spherical mirror performance we upgraded our existing ‘5-rod’ linear Paul trap (shown in figure 4) originally designed by the Monroe group [22]. An aluminium frame supports the four RF quadrupole rods and the two end cap needle electrodes, all made from $0.5\ \text{mm}$ diameter tungsten wire, separated from each other and from the ground by alumina spacers. The needles are electrolytically etched from the cylindrical wire stock. The electrodes are glued to the alumina spacers with a UHV-compatible ceramic adhesive (Scientific Instrument Services, Inc. SCC8). The opposite rod centres are about $1.4\ \text{mm}$ apart, and end caps are separated by about $2\ \text{mm}$.

Our mirror is a commercial-grade aluminium-coated spherical concave $20\ \text{mm}$ radius of curvature, $25\ \text{mm}$ diameter mirror. To fit it into the trap frame which has a $20\ \text{mm}^2$ opening, four edges were ground off. A special aluminium holder was made to keep the mirror normal to the grinding surface to ensure square cut. To fix the mirror to the frame at the desired distance from the ion trap, a precision holder (see figure 4(a)) was made to support the mirror from underneath such that its curvature centre is $10\ \text{mm}$ above the needles. The holder was fixed to the frame by four screws and its alignment was fine-tuned in the transverse direction by moving along

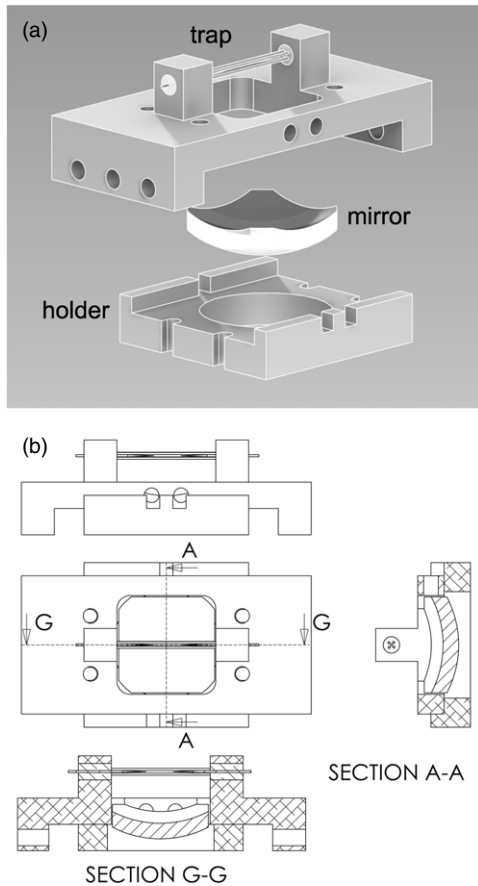


Figure 4. Linear ion trap with integrated spherical mirror. (a) An exploded view of the assembly setup. The mirror holder allows precision positioning of the mirror with respect to the trap. (b) Technical drawing showing the details of the assembly. Dimensions are available upon request.

two knife edges. The alignment procedure was done under a measurement microscope to achieve better accuracy. The needles were placed at an equal distance (about 1 mm) away from the geometric centre. However, after being glued into place the trap assembly apparently shifted with respect to the mirror, moving the trapping centre about $50 \mu\text{m}$ away from the focal point of the mirror.

The trap and the mirror were mounted inside a Kimball Physics, Inc. 4-1/2" Conflat spherical octagon vacuum chamber with four 1.33" Conflat view ports used for laser access, and one 3.1 mm thick, 1.5" re-entrant fused silica view port for ion imaging. To load barium ions into the trap, a simple oven filled with metallic Ba was installed near the trap. The oven is made of a 1 mm diameter alumina tube sealed on one end, and the other end pointing at the trap, with thin tungsten wire wrapped around. The oven can easily be heated up to a few hundred degrees C by running about 1 A of current through the tungsten filament. To collimate the atomic barium beam and prevent barium coating of sensitive trap surfaces and the view ports, a 1 mm aperture was placed between the oven and the trap. A 20 l/s ion pump and a Ti sublimation pump maintain an ultrahigh vacuum (better than 10^{-10} torr) around the trap. The trap is driven by an RF voltage with a few hundred volts amplitude at about 22 MHz generated by a

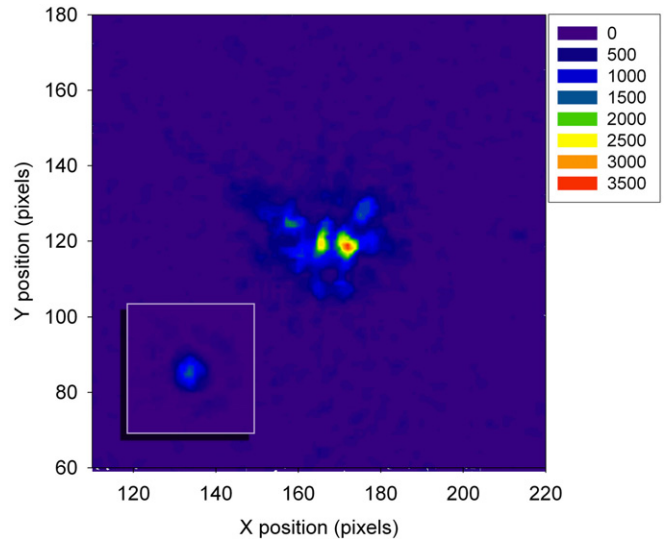


Figure 5. Single Ba⁺ ion image taken by the EMCCD camera using the 0.9 N.A. spherical mirror, compared to the image of the same ion by a 0.25 N.A. multi-element lens with a total magnification of 70 (inset). Exposure time was 0.8 s for both images. The pixel size is $10 \mu\text{m}$. The image intensity is in the (same) arbitrary units. The integrated intensity of the ion image by mirror is about 7.5 times higher than that by multi-element lens.

high- Q helical resonator [23] fed by about 1 W of RF; the end caps are kept at +100 V dc. This produces a trapping potential with the transverse secular motion frequencies $\omega_{x,y}/2\pi \approx 1$ MHz and the axial frequency $\omega_a/2\pi$ of about 100 kHz.

We load Ba ions into the trap by photoionizing [24] neutral barium with a deuterium lamp. The lamp has significant ultraviolet spectral content near 238 nm, which is the ionization threshold for neutral barium. We find that this direct photoionization is very efficient and we are able to load ions with very low Ba oven temperatures.

Barium ions are laser-cooled on the strong $6S_{1/2}-6P_{1/2}$ transition near 493 nm, with an additional laser near 650 nm for repumping out of the metastable $5D_{3/2}$ state. A detailed description of the laser system can be found in [25].

4. Preliminary results

We first set up the imaging system in a way similar to our standard setup. A long working distance, 0.25 N.A. homebuilt multi-element lens designed after [21] was used to form an intermediate image of the ion. A spatial filter (0.5 mm pinhole) was placed in the image plane to reduce the background light including any reflection from the mirror. The intermediate image was then reimaged onto an electron-multiplying CCD (EMCCD) camera (AndorTM Luca^{EM}) with a 25 mm focal length doublet lens.

A narrow-band, 493 nm interference filter was placed in front of the camera to reduce the background even further. The trap was shown to work remarkably well, holding single ions for several days even without the laser cooling, in an excellent agreement with our electric field modelling. An image of a single laser-cooled Ba⁺ ion generated by this system is shown in the inset of figure 5.

In a preliminary test run, we attempted to image the ion onto an EMCCD camera with the spherical mirror alone (i.e., without using any corrector element or the microscope objective). To our surprise we found a very sharp image of a single ion about 60 cm from the mirror (figure 5). It is from this observation that we conclude that the trap centre moved away from the mirror surface during the assembly of the trap. The distorted image shape is probably due to a combination of the spherical aberration and the coma due to a misalignment of the ion location with the optical axis of the mirror. The observed increase in the photon count rate of a factor of about 7.5 was not as good as we expected from the relative ratio (approximately 15) of the solid angles of the 0.9 N.A. and 0.25 N.A. optics, probably because of the large spherical aberration. A large fraction of the light emitted by the ion is actually diffused around the bright image spot, and falls outside the photon-counting aperture. The background (which was subtracted by the camera control software) was rather high due to lack of spatial filtering.

5. Conclusions

In summary, we built and successfully operated a linear Paul trap with an integrated spherical mirror and directly imaged and resolved single ions without any additional optics. A future improvement for correcting spherical aberration with an aspheric lens is proposed and analysed. With these simple and inexpensive modifications we hope to increase the trapped ion fluorescence collection efficiency by more than an order of magnitude.

Acknowledgments

We would like to thank Nathan Pegram for help with early parts of this work and Edan Shahar, Aaron Avril, Chris Dostert, Frank Garcia and Thomas Reicken for their assistance. This research was supported by the National Science Foundation Grant No. 0758025, the Army Research Office, and the University of Washington Royalty Research Fund.

References

- [1] Haffner H, Roos C F and Blatt R 2008 Quantum computing with trapped ions *Phys. Rep.* **469** 155
- [2] Blinov B B, Leibfried D, Monroe C and Wineland D J 2004 Quantum computing with trapped ion hyperfine qubits *Quant. Inf. Proc.* **3** 45
- [3] Blatt R, Haffner H, Roos C F, Becher C and Schmidt-Kaler F 2004 Ion trap quantum computing with Ca⁺ ions *Quant. Inf. Proc.* **3** 61
- [4] Blatt R and Zoller P 1988 Quantum jumps in atomic systems *Eur. J. Phys.* **9** 250
- [5] Turchette Q A, Wood C S, King B E, Myatt C J, Leibfried D, Itano W M, Monroe C and Wineland D J 1998 Deterministic entanglement of two trapped ions *Phys. Rev. Lett.* **81** 3631
- [6] Leibfried D *et al* 2005 Creation of a six-atom ‘Schrödinger cat’ state *Nature* **438** 639
- [7] Haffner H *et al* 2005 Scalable multiparticle entanglement of trapped ions *Nature* **438** 643
- [8] Shor P W 1995 Scheme for reducing decoherence in quantum computer memory *Phys. Rev. A* **52** R2493
- [9] Steane A 1996 Multiple-particle interference and quantum error correction *Proc. R. Soc. A* **452** 2551
- [10] Maunz P, Moehring D L, Olmschenk S, Younge K C, Matsukevich D N and Monroe C 2007 Quantum interference of photon pairs from two remote trapped atomic ions *Nat. Phys.* **3** 538
- [11] Eschner J, Raab Ch, Schmidt-Kaler F and Blatt R 2001 Light interference from single atoms and their mirror images *Nature* **413** 495
- [12] Koo K, Sudbery J, Segal D M and Thompson R C 2004 Doppler cooling of Ca⁺ ions in a Penning trap *Phys. Rev. A* **69** 043402
- [13] Miller R, Northup T E, Birnbaum K M, Boca A, Boozer A D and Kimble H J 2005 Trapped atoms in cavity QED: coupling quantized light and matter *J. Phys. B: At. Mol. Opt. Phys.* **38** S551
- [14] Maunz P, Puppe T, Schuster I, Syassen N, Pinkse P W H and Rempe G 2004 Cavity cooling of a single atom *Nature* **428** 50
- [15] Keller M, Lange B, Hayasaka K, Lange W and Walther H 2004 Continuous generation of single photons with controlled waveform in an ion-trap cavity system *Nature* **431** 1075
- [16] Herskind P, Dantan A, Langkilde-Lauesen M B, Mortensen A, Sorensen J L and Drewsen M 2008 Loading of large ion Coulomb crystals into a linear Paul trap incorporating an optical cavity *Appl. Phys. B* **93** 373–9
- [17] Sondermann M, Maiwald R, Konermann H, Lindlein N, Peschel U and Leuchs G 2007 Design of a mode converter for efficient light-atom coupling in free space *Appl. Phys. B* **89** 489
- [18] Flatt B *et al* 2007 A linear RFQ ion trap for the enriched Xenon observatory *Nucl. Instrum. Methods Phys. Res. A* **578** 399
- [19] Griffiths D J 1999 *Introduction to Electrodynamics* (Englewood Cliffs, NJ: Prentice Hall) p 121
- [20] Born M and Wolf E 1997 *Principles of Optics: Electromagnetic Theory of Propagation, Interference, and Diffraction of Light* (Cambridge: Cambridge University Press) p 276
- [21] Alt W 2002 An objective lens for efficient fluorescence detection of single atoms *Optik* **113** 142
- [22] Blinov B B, Kohn Jr R N, Madsen M J, Maunz P, Moehring D L and Monroe C 2006 Broadband laser cooling of trapped atoms with ultrafast laser pulses *J. Opt. Soc. Am. B* **23** 1170
- [23] MacAlpine W W and Schildknecht R O 1959 Coaxial resonators with a helical inner core *Proc. IRE* **2099**
- [24] Steele A V, Churchill L R, Griffin P F and Chapman M S 2007 Photoionization and photoelectric loading of barium ion traps *Phys. Rev. A* **75** 053404
- [25] Kurz N, Dietrich M R, Shu G, Bowler R, Salacka J, Mirgion V and Blinov B B 2008 Measurement of the branching ratio in the 6P_{3/2} decay of Ba II with a single trapped ion *Phys. Rev. A* **77** 060501